Current Applied Physics 13 (2013) S2–S13

Contents lists available at SciVerse ScienceDirect

Current Applied Physics

journal homepage: www.elsevier.com/locate/cap

Review paper: Toward highly efficient quantum-dot- and dye-sensitized solar cells

Hongsik Choi, Changwoo Nahm, Jongmin Kim, Chohui Kim, Suji Kang, Taehyun Hwang, Byungwoo Park*

WCU Hybrid Materials Program, Department of Materials Science and Engineering, Research Institute of Advanced Materials, Seoul National University, Seoul 151-744, Republic of Korea

ARTICLE INFO

Article history:
Received 28 September 2012
Accepted 17 January 2013
Available online 14 February 2013

Keywords:
Sensitized solar cell
Interface control
Light harvesting
Tandem solar cell

ABSTRACT

Dye- and quantum-dot-sensitized solar cells have attracted tremendous attention as one of the potential low-cost alternatives for *p*–*n* junction silicon solar cells. However, the conversion efficiencies of sensitized solar cells are still lower than those of silicon-based solar cells. Numerous research efforts have been made to enhance the sensitized solar cell efficiency over the past decades. Among the various attempts to improve the photovoltaic properties, the control of interface for reducing the charge recombination and the smart management of the light harvesting have proven to be most effective. Moreover, the *p*–*n* junction structure can offer higher open-circuit voltage than the conventional *n*-type sensitized solar cell. In this review paper, recent developments in sensitized solar cells and the underlying mechanisms will be briefly introduced.

1. Introduction

The vast uses of fossil fuels, causing environmental pollution and global warming, have led us to focus on the renewable energy sources for the future [1,2]. Among the renewable energy sources, solar cells have attracted a great interest as a solution to this situation [3–5]. To date, the silicon-based photovoltaic devices have power-conversion efficiencies over 20% [6]. However, the issues of high cost and environmentally-harmful waste in the processing technologies of silicon-based solar cells should be resolved [7].

Dye-sensitized solar cells (DSSCs) have been considered as one of the most promising photovoltaic technologies because they are generally made from inexpensive and nontoxic components, and can be designed in a diversity of colors and transparencies [8–11]. Since the pioneering work of Grätzel and O'Regan in 1991 [9], tremendous efforts have been made to improve the performance of DSSCs. However, the development of DSSCs has been sluggish over the last ten years, with the highest record of 12% ever reported [12]. To overcome the limited DSSCs efficiency, inorganic semiconductors have been considered as ideal next-generation sensitizers because of their bandgap tunability by controlling the quantum-dot size and high absorption coefficient (10^5–10^6/M cm) [13–16]. Moreover, quantum dots can generate more than two electrons from a single photon when they absorb light with higher energy than the bandgap of quantum dot (multiple-carrier generation) [17]. This may open up the possibility for exceeding the Schottky–Queisser limit. Nevertheless, the achieved conversion efficiencies of quantum-dot-sensitized solar cells (QDSCs) have been ~5% so far [18–21].

One of the main reasons for the efficiency deterioration in QDSC is the charge recombination, caused by porous nature of working electrode. In the conventional construction of sensitized solar cells, the charge recombination takes place dominantly at three possible interfaces: working electrode/electrolyte, quantum-dot-sensitizer/electrolyte, and transparent-conducting oxide (TCO)/electrolyte. Therefore, the control for these interfaces is the key issue for enhancing charge collection efficiencies. To reduce interfacial recombination, nanoscale coating with various materials on the surface of working electrode [22–33], quantum-dot semiconductor [34–38], and/or TCO [39–55] has been proven as an effective method. These nanoscale-passivation ideas have been effectively explored in the field of Li-ion batteries [56–84] and low-temperature fuel cells [85–98].

Another approach to improve efficiency of solar cell is light managements by utilizing light scatterers [99–105] and surface-plasmon resonances [106–111]. The scattering component modifies the photon paths, and extends the traveling distance of the incident light in the photoelectrodes, thereby enhancing the

* Corresponding author. Tel.: +82 2 880 8319; fax: +82 2 885 9671.
E-mail address: byungwoo@snu.ac.kr (B. Park).

1567-1739/$ – see front matter © 2013 Elsevier B.V. All rights reserved.
http://dx.doi.org/10.1016/j.cap.2013.01.023

probability of photons being captured by the sensitizers. Metal nanoparticles can also contribute to the effective light absorption, both by field enhancement through the localized surface-plasmon resonance and by light scattering leading to prolonged optical-path lengths [112–115].

Meanwhile, *p*-type sensitized solar cell, which is the inverse mode of *n*-type counterpart, has attracted much attention as a component for the tandem DSSCs [116–120]. The combination of an *n*-type photoanode (TiO_2) with a *p*-type photocathode (NiO), in a tandem configuration can offer improved open-circuit voltage (V_{oc}). Generally, theoretical efficiency of tandem DSSCs is reported to be ~43%, well beyond that of single-junction DSSCs (~31%) [121–123].

This paper highlights recent progresses in sensitized solar cell in pursuit of the high conversion efficiency. Especially, this article focuses mainly on the nanoscale surface modification with various materials, light-harvesting management with scattering layer and surface-plasmon resonance, and tandem-sensitized solar cells.

2. Interface control for reducing charge recombination

2.1. Transparent-conducting-oxide/electrolyte interface

In DSSCs and QDSCs, the TiO_2 compact layer has been used to prevent the backward electron transfer from TCO to the electrolyte [41–47]. My group reported the correlations between photovoltaic properties and $TiCl_4$-treated compact-layer thickness in DSSCs system [41]. The physically-blocked FTO/electrolyte interface effectively prohibits injected electrons in FTO from recombining with the redox couple in electrolyte. As shown in Fig. 1, higher V_{oc} is obtained compared to the bare cell, and the short-circuit current (J_{sc}) is also increased. In particular, the 25 nm-deposited cell exhibits ~32% increase in power-conversion efficiency compared to the bare cell. In case of the thicker compact layer, however, the power-conversion efficiency is decreased. The trap states present in the thicker TiO_2 compact layer account for this phenomenon because these trap states tend to block the pathway of photoexcited electrons from the nanoporous TiO_2 layer to the FTO electrode [124,125].

The suppressed charge recombination at the FTO/electrolyte interface was analyzed by the open-circuit voltage decay, as shown in Fig. 2(a). The slow decay responses of the TiO_2 compact layer indicates that the recombination between electrons in the FTO and I_3^- in the electrolyte is drastically reduced by the TiO_2 compact layer. From the voltage decay curves, the electron-carrier lifetime (τ) can be calculated as a function of voltage [126,127], and the corresponding electron-carrier lifetime of DSSCs is shown in Fig. 2(b). At all voltages, electron-carrier lifetime of the 25 nm-deposited cell is approximately five times higher compared with the bare cell.

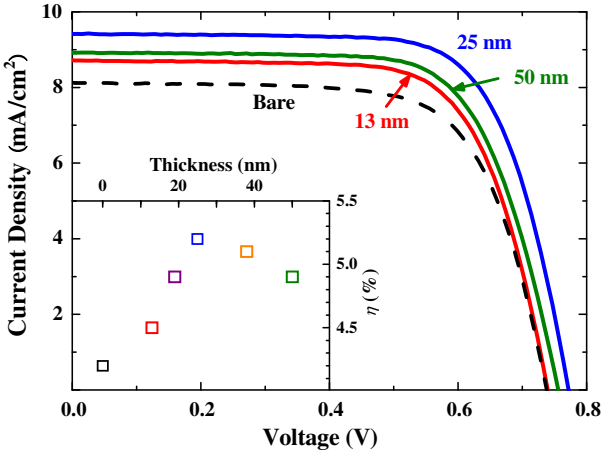

Fig. 1. Photocurrent–voltage curves of DSSCs with various TiO_2 compact-layer thicknesses. The inset shows power-conversion efficiency of DSSCs as a function of the compact-layer thickness. Reprinted with permission from B. Park et al. [41]. Copyright 2012, Elsevier.

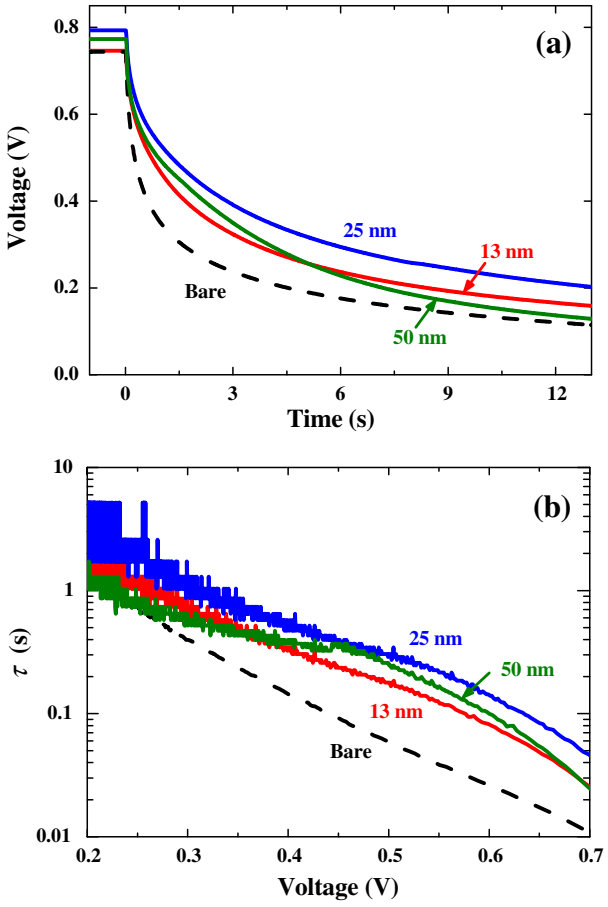

Fig. 2. (a) Experimental decay results of V_{oc} for the bare and compact-layer coated DSSCs. (b) Electron lifetimes as a function of voltage. Reprinted with permission from B. Park et al. [41]. Copyright 2012, Elsevier.

In the case of QDSCs system, the compact layer can also effectively reduce the backward reaction at the FTO/polysulfide-electrolyte interface. However, different from DSSCs system, asymmetric enhancement of incident photon-to-current conversion efficiency (IPCE) is observed for the thicker compact-layer cell (Fig. 3) [53]. In the case of DSSCs, an IPCE near the UV region is mainly affected by the absorption from TiO_2 electrode, because of higher molar absorption coefficient of TiO_2 than that of dye molecules (~10^4/M cm) [128]. In contrast, the CdS quantum dots have similar molar absorption coefficients (10^5–10^6/M cm), therefore, the values of the IPCE are represented by the sum of the CdS and TiO_2 responses in the UV region. As a result, the thicker compact-layer cell shows lower IPCE value below the ~390 nm region compared to the bare cell. Furthermore, the slopes of the IPCE spectra become steeper below the bandgap energy (middle region), since more trap states exist in the thicker compact layer meaning increased absorption near the conduction band. In the higher wavelength region, symmetric enhancement of the IPCE is observed because the absorption through the TiO_2 compact layer becomes negligible, and electron recombination at the FTO/

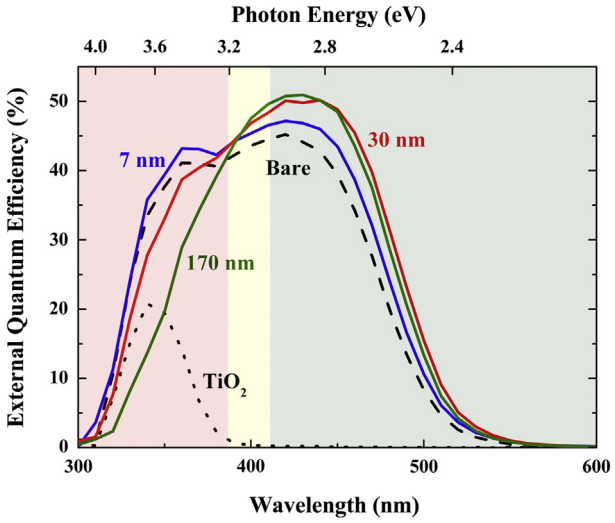

Fig. 3. Incident photon-to-current conversion efficiency (IPCE) spectra of QDSCs with various blocking-layer thicknesses. The IPCE of TiO_2 nanoparticles without CdS sensitizer is shown as a dotted line. Reprinted with permission from B. Park et al. [53]. Copyright 2011, Elsevier.

electrolyte interfaces is effectively suppressed. The thickness effects of TiO_2 compact layer in QDSCs are summarized in Fig. 4.

Another approach to minimize leakage electrons at TCO/electrolyte interface is to introduce potential-barrier layer such as Nb_2O_5, as shown in Fig. 5. Yanagida's group reported that nanoscale Nb_2O_5 layer worked as a remarkable blocking layer when deposited by rf magnetron sputtering [48]. Fig. 6 presents the *J–V* curve of the interface-optimized DSSCs by Nb_2O_5 blocking layer under AM 1.5 illumination. The metal oxide blocking layer can remarkably decrease the dark current (without illumination), resulting in higher V_{oc} and J_{sc} under AM 1.5 compared with the bare cell.

2.2. TiO_2-nanoparticle-electrode/electrolyte and quantum-dot-sensitizer/electrolyte interfaces

For the efficient operation of DSSCs and QDSCs, recombination pathways occurring at the TiO_2/sensitizer/electrolyte interface should also be minimized. The energy band structure at the TiO_2/dye-sensitizer interface is illustrated in Fig. 7 where charge separation processes take place in DSSCs. The generated electrons are able to recombine either with oxidized dye (path (3)) or redox couple (path (5)). In order to reduce these backward reactions, the passivation layer should have wide bandgap and conduction

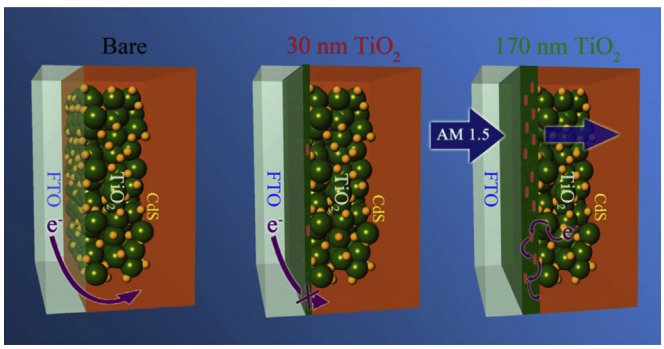

Fig. 4. Schematic figures of the TiO_2 blocking-layer effects on the performance of CdS-sensitized solar cells. Reprinted with permission from B. Park et al. [53]. Copyright 2011, Elsevier.

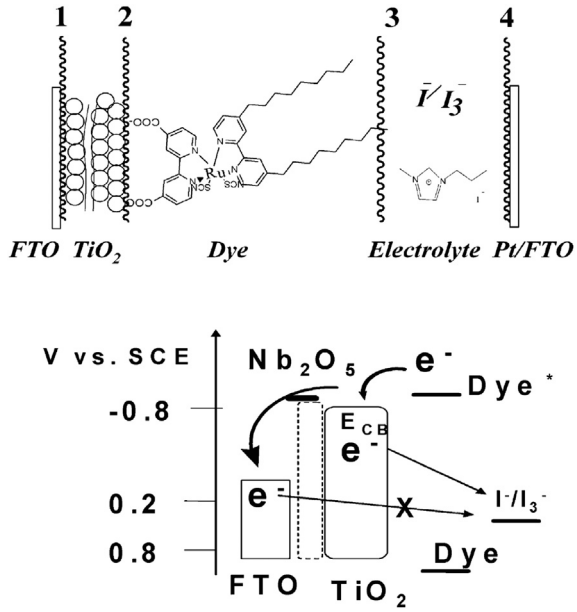

Fig. 5. Schematic views of interfaces in the DSSC device and the electron transfer of the FTO/Nb_2O_5/TiO_2 electrode. Reprinted with permission from S. Yanagida et al. [48]. Copyright 2007, Royal Society of Chemistry.

bandedge above that of TiO_2. At the same time, the surface charge of passivation layer is also important for the attachment of dye. Considering electrostatic interactions between dye and the passivation layer makes several metal oxides (e.g., ZnO, $CaCO_3$, MgO, and Al_2O_3) more charming, because they bear more positive surface charges than TiO_2, as shown in Fig. 8(a) [22–28].

The effect of Al_2O_3 coating layer thickness on the device performance was examined by varying the number of ALD cycles [27]. The high-resolution transmission electron microscope (HR-TEM) images of ALD samples after 20 and 40 cycles are shown in Fig. 9, respectively. These reveal the uniform shell formation around TiO_2 nanoparticles with a relatively-uniform alumina layer. With increasing number of Al_2O_3 coating cycles, a large increase in J_{sc}, V_{oc}, and the fill factor, thus enhancement in efficiency is observed up to 20 cycles (Fig. 10(a)). The increase in efficiency is likely to arise from an abundant adsorption of dye (Fig. 8(b)), and reduced carrier recombination at the TiO_2/dye/electrolyte interface.

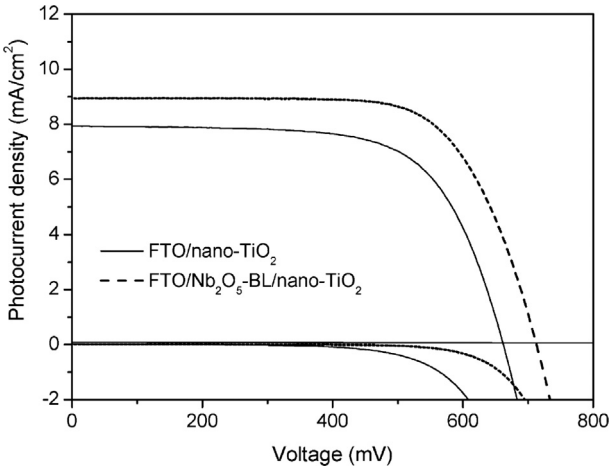

Fig. 6. *J–V* curves of cells employing Z-907 sensitized FTO/TiO_2 (solid line) and FTO/Nb_2O_5/TiO_2 electrodes (dashed line) under AM 1.5 illumination. Reprinted with permission from S. Yanagida et al. [48]. Copyright 2007, Royal Society of Chemistry.

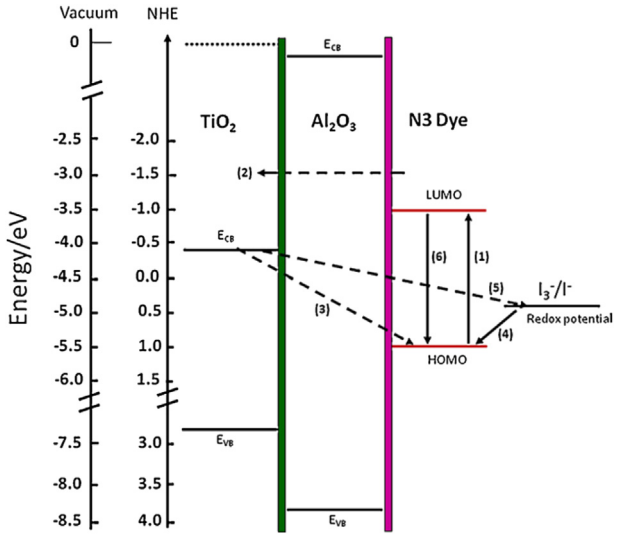

Fig. 7. Schematic diagram of band structure including interfacial charge-transfer processes occurring at TiO_2/dye/electrolyte interface in DSSCs. Reprinted with permission from S.-W. Rhee et al. [27]. Copyright 2010, Elsevier.

The improvement in photo-voltage is attributed to a reduction in dark current of the cells with Al_2O_3 layers, as shown in Fig. 10(b). The J_{SC} and V_{OC}, however, drop sharply as the coating thickness increases. This clearly indicates that the thickness of Al_2O_3 has

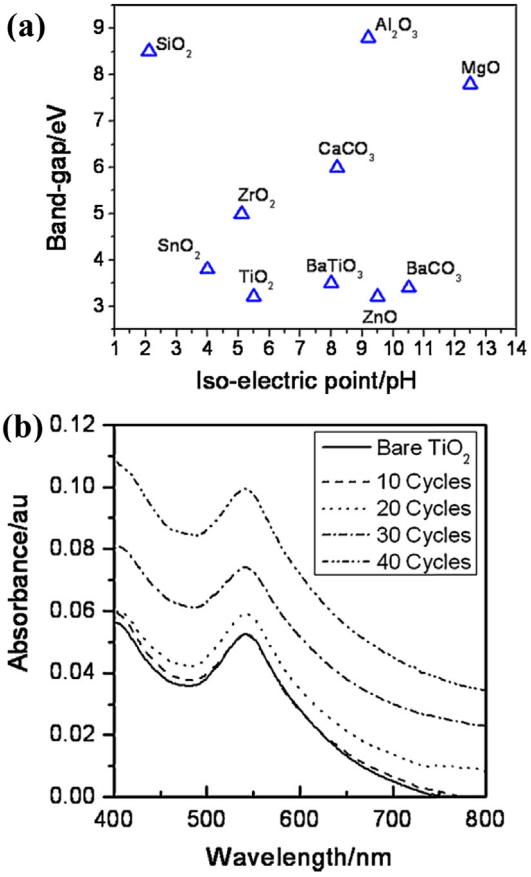

Fig. 8. (a) Graphical representation of isoelectric point and bandgap of various oxide materials. (b) Absorbance spectra of dye desorbed from bare and alumina-coated TiO_2 samples using 0.1 M NaOH. Alumina was deposited by ALD process with deposition cycles between 10 and 40. Reprinted with permission from S.-W. Rhee et al. [27]. Copyright 2010, Elsevier.

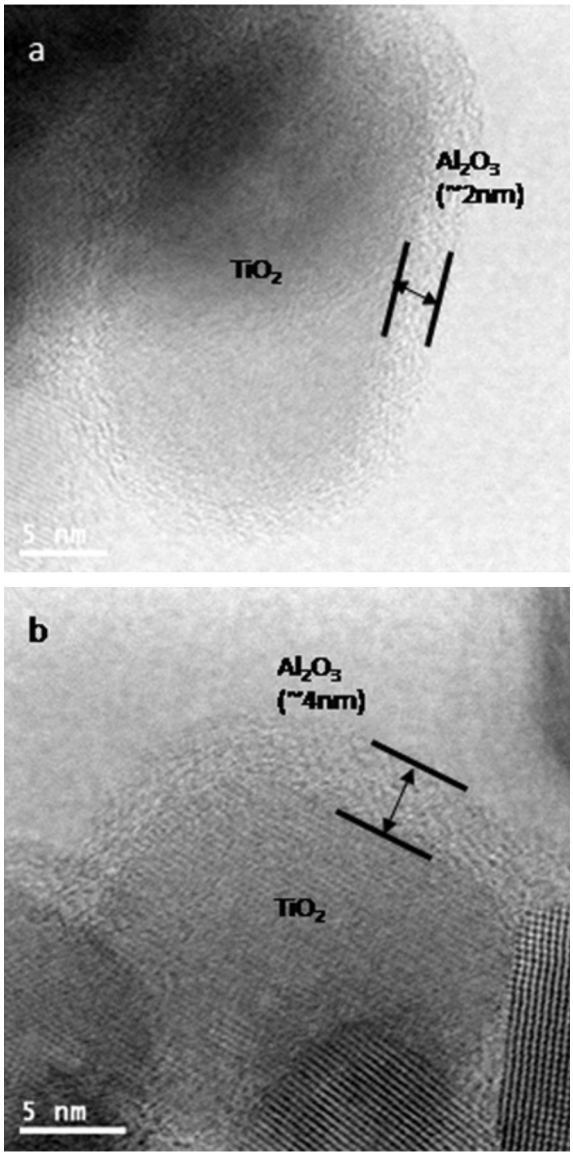

Fig. 9. High-resolution TEM images of TiO_2 porous layer covered with ALD alumina deposited with (a) 20 cycles and (b) 40 cycles. Reprinted with permission from S.-W. Rhee et al. [27]. Copyright 2010, Elsevier.

exceeded the tunneling thickness (~2 nm), and thereby leads to a decrease in device performance. Although the amount of dye adsorption is higher in the thicker Al_2O_3 layer (~4 nm), it results in the poor cell performance because the thick Al_2O_3-barrier blocks electron transport into TiO_2.

In case of the QDSCs system, surface modification of the TiO_2/electrolyte and quantum-dot/electrolyte interfaces is also crucial for high efficiency. My group reported the role of nanoscale TiO_2 passivation on the TiO_2-nanoparticle electrode for the performance of CdS–QDSCs [32]. As shown in Fig. 11, the optimized coating layer enhances the power-conversion efficiency by ~40% compared with the bare CdS-sensitized solar cell. The enhanced efficiency by TiO_2 passivation on the TiO_2 electrode is attributed to the reduction of charge recombination at the TiO_2/CdS/polysulfide-electrolyte interfaces by passivating the surface defects on the TiO_2-nanoparticle layer, as shown in Fig. 12. The effective suppression of recombination was confirmed by impedance analysis at the open-circuit voltage under AM 1.5 illumination (Fig. 13(a)). The charge-transfer resistance shows higher values with $TiCl_4$ treatment,

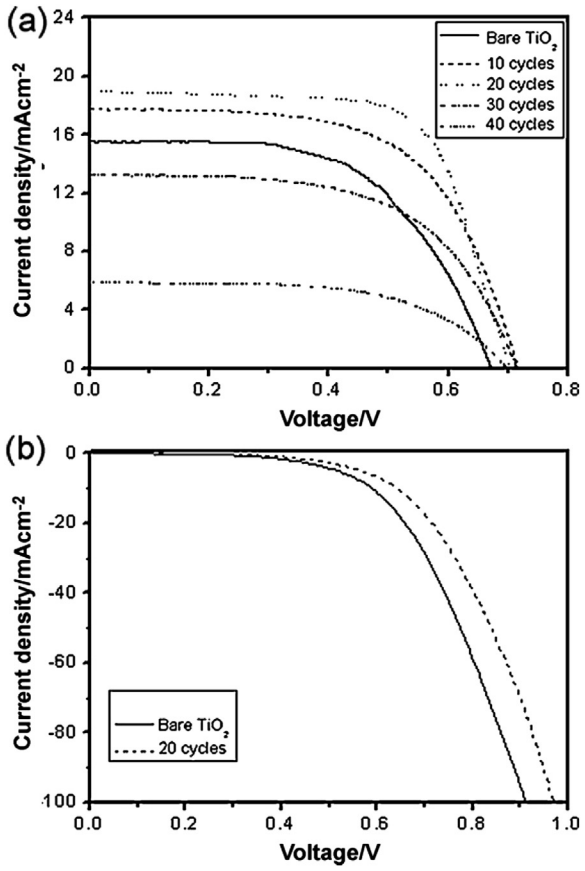

Fig. 10. (a) *J–V* characteristics of solar cell with bare and alumina-coated TiO_2 samples measured under one sun illumination. (b) *J–V* curves of bare TiO_2 and 20 cycles alumina-coated sample measured in dark. Reprinted with permission from S.-W. Rhee et al. [27]. Copyright 2010, Elsevier.

which means that the TiO_2-coating layer effectively suppresses charge transfer at the TiO_2/electrolyte interface.

As distinct from DSSCs, electrolyte diffusion is one of the factors to consider for the performance of QDSCs. This is because the diffusivity of polysulfide electrolyte without TiO_2 nanoparticles ($\sim 10^{-6}$ cm^2/s) is approximately 2 orders of magnitude lower than that of the iodide electrolyte typically used in DSSCs ($\sim 10^{-4}$ cm^2/s)

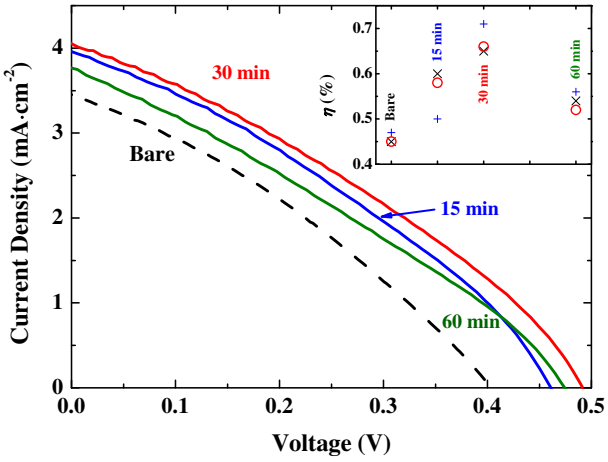

Fig. 11. Photocurrent–voltage curves of CdS quantum-dot-sensitized solar cells with various TiO_2-coating times. The inset shows power-conversion efficiency of QDSCs as a function of the coating time. Reprinted with permission from B. Park et al. [32]. Copyright 2012, Elsevier.

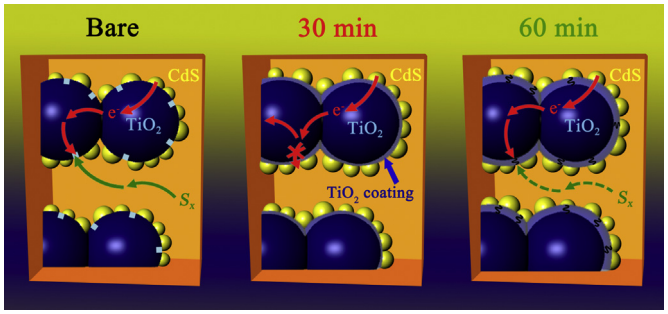

Fig. 12. Schematic figures of the $TiCl_4$-treatment effects on the performance of CdS-sensitized solar cells. Reprinted with permission from B. Park et al. [32]. Copyright 2012, Elsevier.

[129], and the size of quantum-dot sensitizer (2–6 nm) is larger than that of a dye molecule (~1 nm) [128]. From the impedance measured under dark condition [130,131], the diffusivity of electrolyte through the nanoporous TiO_2 electrode was obtained (Fig. 13(b)). The decrease in the diffusivity is associated with the increasing amount of TiO_2 on the nanoparticle electrode because the amount of layer scales with the TiO_2-passivation time. As a result, the pore size within TiO_2-nanoparticle film decreases and, therefore, the electrolyte diffusion through nanopores becomes inevitably difficult. This result is consistent with the increase of series resistance at V_{oc} for thicker TiO_2-coated cell (Fig. 11).

A great improvement in photocurrent and conversion efficiency was also reported for QDSCs when the CdS/CdSe-sensitized mesoporous TiO_2 electrode was passivated by ZnS. Lee et al. reported that ZnS layer coated on the TiO_2/CdS/CdSe photoelectrode showed enhanced photovoltaic performance (Fig. 14), due to the passivation of CdSe surface states from the photocorrosion [20]. It was furthermore argued that ZnS layer was able to inhibit the recombination of excited electron at the quantum-dot/electrolyte interface. It should be noted that in order to enhance chemical stability and photovoltaic in QDSCs, the use of nanoscale coatings on the quantum-dot sensitizer is also essential, and further research is necessary for better understanding of the interfacial charge-transport mechanisms.

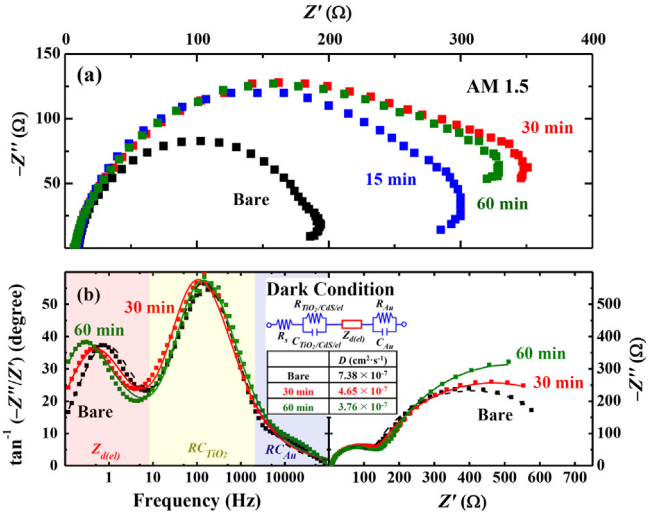

Fig. 13. (a) Electrochemical impedance spectra measured under AM 1.5 illumination, and (b) Bode and Nyquist plots measured under dark conditions with various TiO_2-passivation conditions at V_{oc}. Reprinted with permission from B. Park et al. [32]. Copyright 2012, Elsevier.

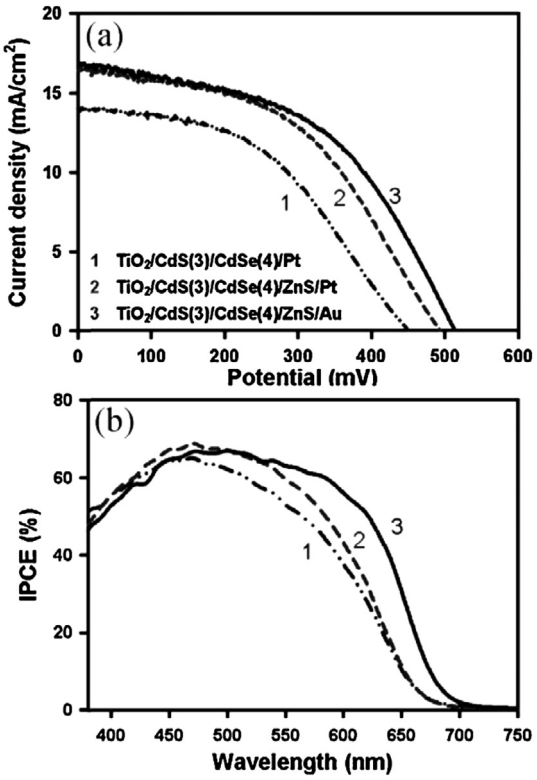

Fig. 14. (a) Effects of ZnS passivation layer and counter electrode on the *J*–*V* characteristics of the TiO_2/CdS/CdSe electrode. (b) Incident photon-to-current conversion efficiency spectra measured as a function of wavelength. Reproduced with permission from Y.-L. Lee and Y.-S. Lo [20]. Copyright 2009, Wiley-VCH.

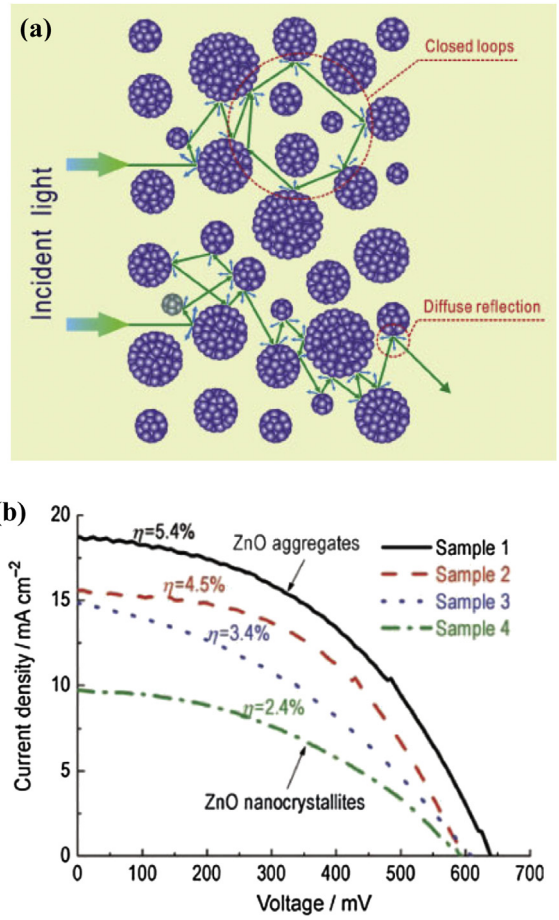

Fig. 15. (a) Schematic of light scattering and photon localization within a film consisting of submicrometer-sized aggregates. (b) Photovoltaic behavior of N_3-dye-adsorbed ZnO-film samples with differences in the degree of nanocrystallite aggregates. Reproduced with permission from G. Cao et al. [103]. Copyright 2009, Wiley-VCH.

3. Improving light-harvesting efficiency

3.1. Light-scattering effect

Optical effects generated by nanostructures provide opportunities for increasing the performance of sensitized solar cell. The light scattering is considered as another approach that can make an impact on the light-harvesting capability of the photoelectrode by utilizing optical enhancement effects. There have been many studies on enhancing the light-harvesting efficiency of photoelectrodes by adding submicrometer-scale particles as light scatterers, resulting in a significant advance in DSSCs. However, the introduction of large-sized particles into nanocrystalline films has unavoidable effect of lowering the internal surface area of the photoelectrode film [101].

Recently, submicrometer-sized polydisperse aggregates consisting of nanosized crystallites have been utilized for efficient scatterers [100–103], while the nanocrystallites provide the films with the necessary nanoporous structure and large surface area, as shown in Fig. 15(a). From the *J*–*V* curves in Fig. 15(b), the conversion efficiency of 5.4% is observed for submicrometer-sized polydisperse aggregates, whereas that of 2.4% is observed for ZnO nanoparticles without submicrometer-sized scatterers. This improved performance of DSSCs can be explained with the significantly extended traveling distance of light within the photoelectrode film.

However, the size of aggregates creates large voids between aggregates in photoelectrode (Fig. 16(a)), and these large voids may result in low connectivity for charge transfer and a decreased electron-diffusion length [132]. Thus, more charge recombination can occur, leading to reduced conversion efficiency. In this respect, Cao's group suggested the use of aggregate/nanoparticle mixtures, as shown in Fig. 16(b) [105]. They have systemically investigated the influences of the aggregate/nanoparticle ratio on the performance of DSSCs. The admixing of TiO_2 aggregates with nanoparticles exhibits an obvious improvement on the performance of DSSCs compared to both pure TiO_2 aggregates (5.35%) and pure TiO_2 nanoparticles (5.80%), as shown in Fig. 17. The TiO_2

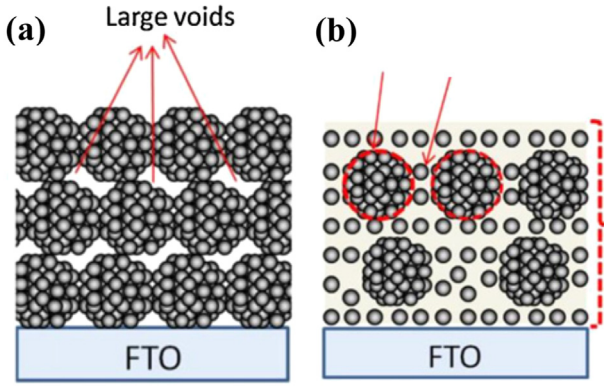

Fig. 16. (a) Films made of nanocrystallite aggregates for both high surface area and light scattering, and (b) with mixed nanoparticles and nanocrystallite aggregates for increased surface area and light scattering. Reprinted with permission from G. Cao et al. [105]. Copyright 2011, Elsevier.

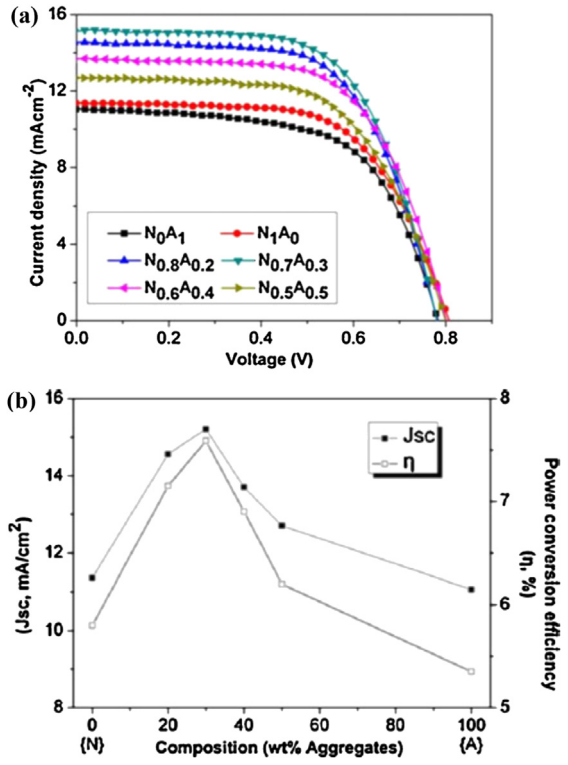

Fig. 17. (a) *J–V* curves of DSSCs with mixed photoelectrodes. (b) Comparison of the short-circuit current density and power-conversion efficiency as a function of TiO_2 nanoparticle (*N*) and aggregate (*A*) fraction. Reprinted with permission from G. Cao et al. [105]. Copyright 2011, Elsevier.

nanoparticles filling large voids among the aggregates lead to the increased amount of dye loading as well as the better connectivity for carrier transport.

3.2. Surface-plasmon resonance

The light-harvesting properties can also be amplified by employing surface-plasmon resonance. Surface plasmons are created when incident light excites oscillations of free electrons in metal nanoparticles, such as gold, aluminum, and silver. Hupp's group investigated the plasmon-enhanced absorption of the dyes by introducing silver nanoparticles [107]. Because the silver nanoparticles are corrosive in iodide electrolyte, they are conformably coated with a protective layer of TiO_2 by ALD (Fig. 18). From the IPCE measurement shown in Fig. 18(a), the cell with both dye and silver

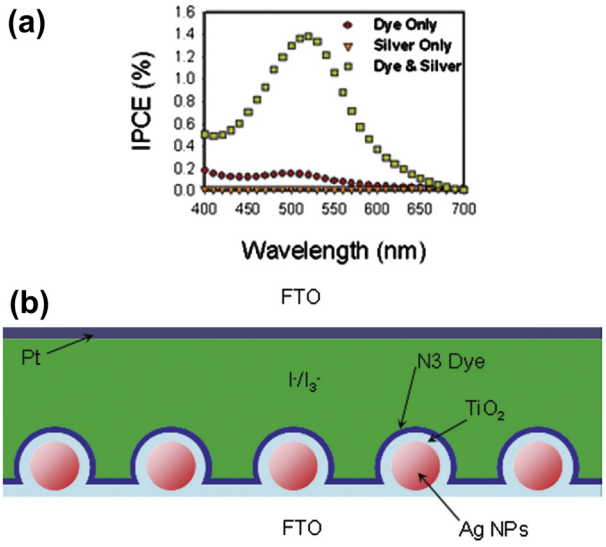

Fig. 18. (a) Incident photon-to-current conversion efficiency spectra of the DSSCs with silver nanoparticles and dye. (b) Configuration of solar cells containing silver nanoparticles and dye. From Ref. [107].

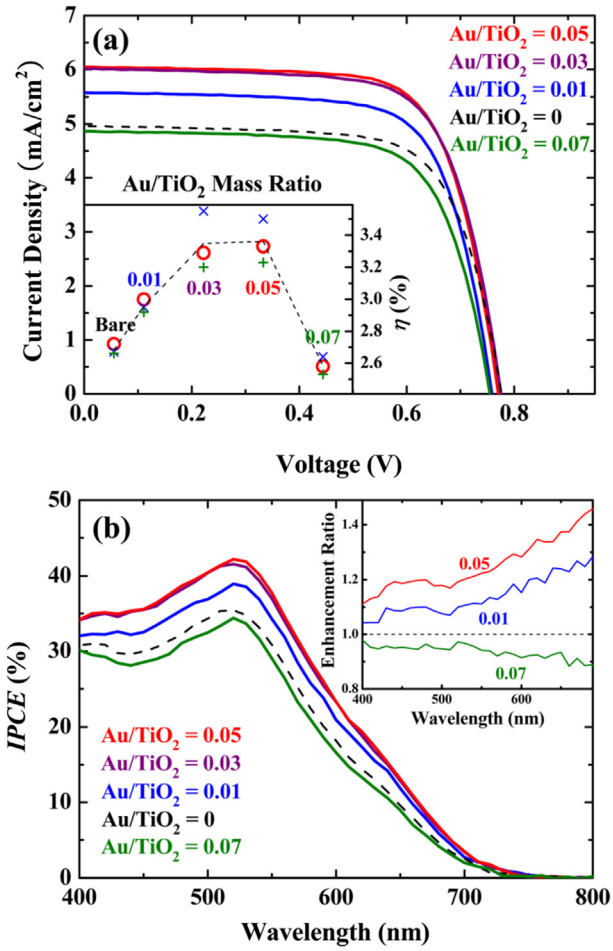

Fig. 19. (a) *J–V* characteristics of DSSCs at various Au/TiO_2 mass ratios. The inset shows the power-conversion efficiency of DSSCs with respect to the Au/TiO_2 mass ratio. (b) Incident photon-to-current conversion efficiency spectra of DSSCs at various Au/TiO_2 mass ratios. The IPCE enhancement ratios are also shown compared with the bare DSSC ($Au/TiO_2 = 0$) in the inset. Reprinted with permission from B. Park et al. [111]. Copyright 2011, American Institute of Physics.

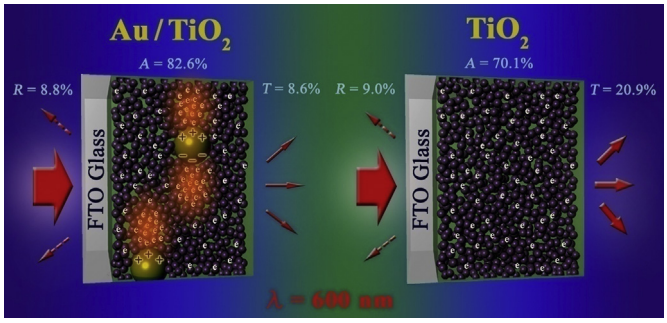

Fig. 20. Schematic figure representing the enhancement of Au/TiO_2-DSSC. Field enhancement near the Au nanoparticles is depicted as orange-color regions. Reprinted with permission from B. Park et al. [111]. Copyright 2011, American Institute of Physics.

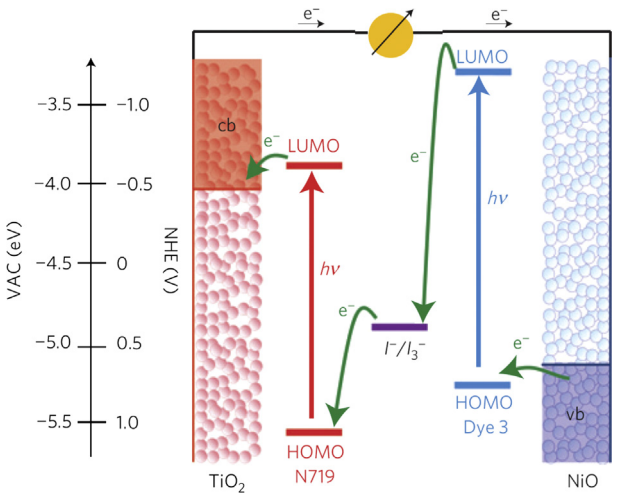

Fig. 21. Scheme for the electron-transfer processes occurring in the tandem-sensitized solar cell. Reprinted with permission from U. Bach et al. [116]. Copyright 2010, Nature Publishing Group.

nanoparticles exhibits higher IPCE peak value (~1.4%) compared to that made of the only dye (~0.2%) or only silver (~0%) samples. These results clearly confirm that spectra overlap between the dye and surface plasmon can give rise to an effective light absorption by the field-enhancement effect.

Recently, less-corrosive gold nanoparticles, as light-harvesting component, are incorporated to DSSCs system, and as a case study, the effects of 100-nm-diameter Au nanoparticles on the solar cell performance were investigated [111]. As shown in Fig. 19, the conversion efficiencies of Au/TiO_2 mixed cells are enhanced, which is mainly attributed to the increased current density. The IPCE enhancement ratio also reveals that the Au/TiO_2 mixed cell absorbs much more photons than the bare cell, particularly in the longer wavelength region (Fig. 19(b)). The electric field of incident light is strongly amplified by the oscillating surface charges in Au nanoparticles, yielding increased light absorption [133,134]. Therefore, more light can be absorbed by dye sensitizers, and more photocurrent can be generated in DSSCs, as shown in Fig. 20.

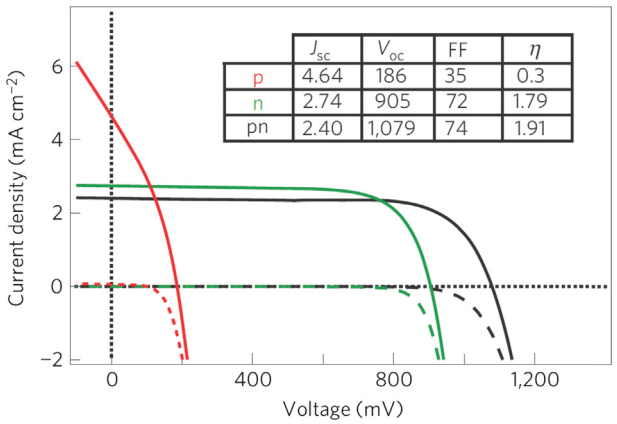

Fig. 22. *J–V* characteristics of a tandem solar cell (black) as well as *p*-type DSSCs (red) and *n*-type DSSCs (green) under illumination (solid lines) and in the dark (dashed lines). (For interpretation of the references to colour in this figure legend, the reader is referred to the web version of this article.) Reprinted with permission from U. Bach et al. [116]. Copyright 2010, Nature Publishing Group.

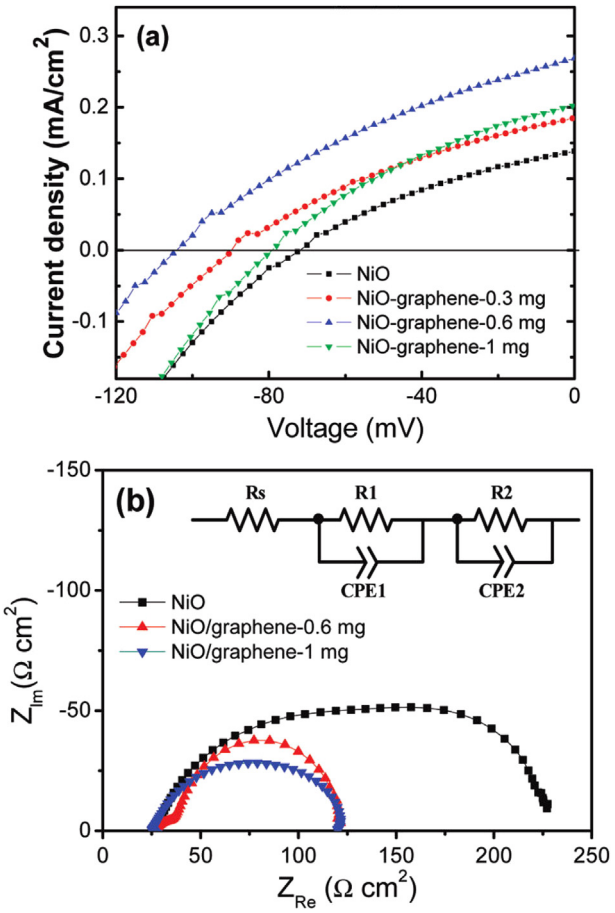

Fig. 23. (a) *J–V* characteristics of *p*-type DSSCs based on NiO and NiO/graphene composite films. (b) Nyquist plots of *p*-type DSSCs based on NiO and NiO/graphene composite electrodes. The inset displays the equivalent circuit of the devices. From Ref. [118].

4. *p*-type sensitized solar cell

4.1. *p–n* junction sensitized solar cell for high open-circuit voltage

Sensitized solar cell systems are generally composed of a nanoporous *n*-type semiconductors, such as TiO_2 and ZnO, coated with photosensitizers acting as an electron donor upon light excitation. In contrast, there is the limited number of studies on the sensitization of *p*-type semiconductors. The photoinjected hole transports into the valence band of the *p*-type semiconductor, of which the operating principle is just inverse scheme of the counterpart (*n*-type). The investigation of *p*-type sensitized solar cells is especially vital for the construction of tandem-sensitized solar cells (DSSCs and QDSCs). A scheme of tandem structure with the approximate energy levels is shown in Fig. 21. The tandem cell consists of a photoanode (*n*-type) and a photocathode (*p*-type) in a sandwich configuration with an intermediate electrolyte [116].

In tandem DSSCs, the maximum open-circuit voltage is determined by the difference between the conduction bandedge of the photoanode and the valence bandedge of the photocathode. The tandem (0.8 μm TiO_2 and 3.3 μm NiO) DSSC structure exhibits the V_{oc} of ~1.08 V, closely matching the sum of V_{oc} for *n*-type DSSC and *p*-type DSSC with similar short-circuit current to that of the *n*-type DSSC (Fig. 22). Therefore, the overall efficiency of tandem cell clearly exceeds that of the only *n*-type DSSC. However, the overall tandem efficiencies [116,121] are still considerably lower than those of conventional TiO_2-based DSSCs [9,10].

4.2. Modifications in p-type sensitized solar cell

The efficiencies of only *p*-type DSSCs are far below 0.5%, which limits the efficiency of tandem DSSCs drastically. Therefore, optimizing the power-conversion efficiency of *p*-type DSSCs is a key issue. As a photocathode, NiO has been widely adopted in that it is known as a large bandgap (3.5 eV) semiconductor with *p*-type nature as synthesized [135–137]. The main reason for the low efficiency in *p*-type DSSCs is that NiO has a low hole diffusivity ($\sim 10^{-8}$ cm^2/s), which may limit the diffusion length of the hole carriers resulting in the loss of photogenerated holes through recombination [138,139]. Several investigations to reduce fast charge recombination in NiO are currently underway as it is one of the major issues for increasing the performance of *p*-type DSSCs [118–120,123].

To improve the charge-transport properties, Yang et al. suggested the NiO/graphene nanocomposite film [118]. Then, the injected holes in the NiO photocathode can be transferred more rapidly through the graphene nanosheets. The enhanced hole transport by graphene gives rise to the improved J_{sc} and V_{oc}, as shown in Fig. 23(a). They analyzed the charge-transfer kinetics in the NiO/graphene nanocomposite films: the semicircle in the middle frequencies ($1–10^2$ Hz) of the Nyquist plot can be assigned to the hole-transport resistance in the nanoporous NiO electrode [140]. As shown in Fig. 23(b), the semicircles for the NiO/graphene electrodes are smaller than those of the bare NiO electrode, confirming that the carrier recombination of the composite-based *p*-type DSSCs is significantly suppressed due to the enhanced hole transport by the presence of conducting graphene.

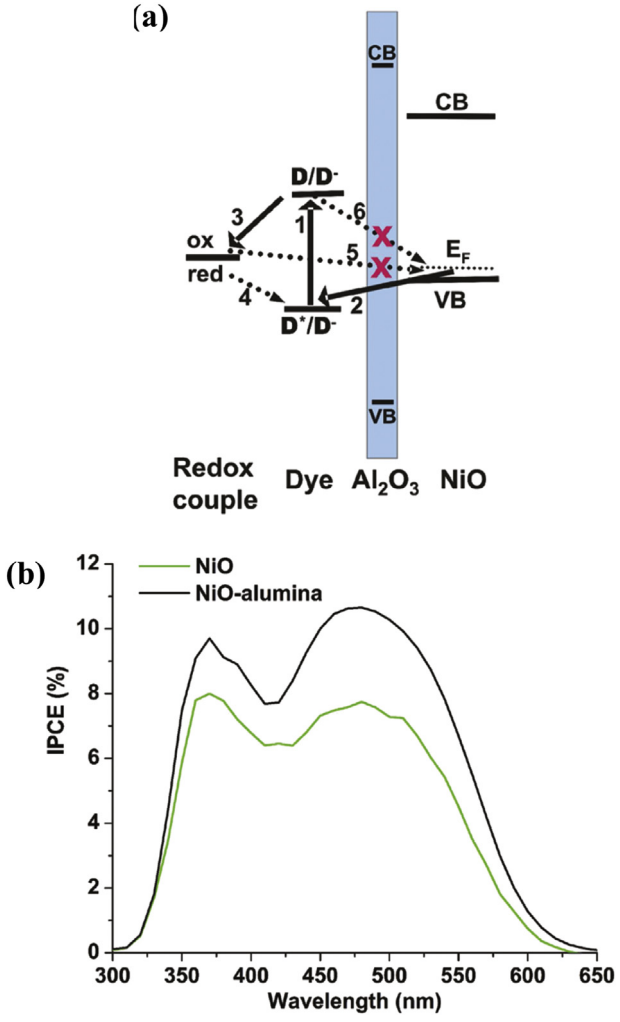

Fig. 24. (a) Schematic representation of the interfacial electron-transfer processes by the alumina-coating effect. (b) IPCE plots of *p*-type DSSCs fabricated from untreated NiO film and from a NiO film treated with 1 ALD cycle of alumina. From Ref. [120].

Another approach for reducing hole recombination is the surface modification of NiO electrode with a nanoscale blocking layer of a wide bandgap material (Fig. 24(a)). In this respect, Wu's group coated porous NiO electrodes with Al_2O_3 by ALD. Even though the amount of adsorbed dye on the NiO–Al_2O_3 film is slightly lower than that on the bare NiO film (different from the DSSCs system with Al_2O_3 coating), Al_2O_3-coated NiO cell exhibits higher collection efficiency of injected holes compared to the bare cell (Fig. 24(b)). This nanoscale Al_2O_3 layer has effectively reduced the hole recombination at the NiO/electrolyte interface.

5. Conclusions

This paper has mainly focused on the various approaches in pursuit of developing highly efficient sensitized solar cells, most of which are devoted to nanoscale surface passivation and tailoring desired nanostructures for light-harvesting efficiency. The basic tactics of enhanced photovoltaic properties rely on the reduced carrier recombination at the various interfaces, improved light absorption by photon management, and construction of tandem structures. It is obvious that exploiting intelligent nanoscience/nanotechnology to overcome these prohibitive issues will be the essential for the future work of quantum-dot- and dye-sensitized solar cells.

Acknowledgments

This research was supported by the National Research Foundation of Korea, through the World Class University (WCU, R31-2008-000-10075-0) and the Korean Government (MEST: NRF, 2010-0029065).

References

[1] J.P. Holdren, Science and technology for sustainable well-being, Science 456 (2008) 424–434.
[2] N. Lior, Energy resources and use: the present situation and possible paths to the future, Energy 33 (2008) 842–857.
[3] P.V. Kamat, Meeting the clean energy demand: nanostructure architectures for solar energy conversion, J. Phys. Chem. C 111 (2007) 2834–2860.
[4] K.W.J. Barnham, M. Mazzer, B. Clive, Resolving the energy crisis: nuclear or photovoltaics, Nat. Mater. 5 (2006) 161–164.
[5] G.J. Meyer, Molecular approaches to solar energy conversion with coordination compounds anchored to semiconductor surfaces, Inorg. Chem. 44 (2005) 6852–6864.
[6] T. Saga, Advances in crystalline silicon solar cell technology for industrial mass production, NPG Asia Mater. 2 (2010) 96–102.
[7] Y. Ooyama, Y. Harima, Molecular designs and syntheses of organic dyes for dye-sensitized solar cells, Eur. J. Org. Chem. (2009) 2903–2934.
[8] N.S. Lewis, Toward cost-effective solar energy use, Science 315 (2007) 798–801.
[9] B. O'Regan, M. Grätzel, A low-cost, high-efficiency solar cell based on dye-sensitized colloidal TiO_2 films, Nature 353 (1991) 737–740.
[10] M. Grätzel, Solar energy conversion by dye-sensitized photovoltaic cells, Inorg. Chem. 44 (2005) 6841–6851.
[11] Z. Ning, Y. Fu, H. Tian, Improvement of dye-sensitized solar cells: what we know and what we need to know, Energy Environ. Sci. 3 (2010) 1170–1181.
[12] A. Yella, H.-W. Lee, H.N. Tsao, C. Yi, A.K. Chandiran, M.K. Nazeeruddin, E.W.-G. Diau, C.-Y. Yeh, S. Zakeeruddin, M. Grätzel, Porphyrin-sensitized solar cells with cobalt (II/III)-based redox electrolyte exceed 12 percent efficiency, Science 334 (2011) 629–633.
[13] S. Ruhle, M. Shalom, A. Zaban, Quantum-dot-sensitized solar cells, ChemPhysChem 11 (2010) 2290–2304.
[14] G. Hodes, Comparison of dye- and semiconductor-sensitized porous nanocrystalline liquid junction solar cells, J. Phys. Chem. C 112 (2008) 17778–17787.

[15] R.J. Ellingson, M.C. Beard, J.C. Johnson, P. Yu, O.I. Micic, A.J. Nozik, A. Shabaev, A.L. Efros, Highly efficient multiple exciton generation in colloidal PbSe and PbS quantum dots, Nano Lett. 5 (2005) 865–871.

[16] D.-R. Jung, J. Kim, B. Park, Surface-passivation effects on the photoluminescence enhancement in ZnS:Mn nanoparticles by ultraviolet irradiation with oxygen bubbling, Appl. Phys. Lett. 96 (2010) 211908.

[17] J.B. Sambur, T. Novet, B.A. Parkinson, Multiple exciton collection in a sensitized photovoltaic system, Science 330 (2010) 63–66.

[18] J. Xu, X. Yang, Q.-D. Yang, T.-L. Wong, S.-T. Lee, W.-J. Zhang, C.-S. Lee, Arrays of CdSe sensitized ZnO/ZnSe nanocables for efficient solar cells with high open-circuit voltage, J. Mater. Chem. 22 (2012) 13374–13379.

[19] V. Gónzalez-Pedro, X. Xu, I. Mora-Seró, J. Bisquert, Modeling high-efficiency quantum dot sensitized solar cells, ACS Nano 4 (2010) 5783–5790.

[20] Y.-L. Lee, Y.-S. Lo, Highly efficient quantum-dot-sensitized solar cell based on co-sensitization of CdS/CdSe, Adv. Funct. Mater. 19 (2009) 604–609.

[21] J.A. Chang, J.H. Rhee, S.H. Im, Y.H. Lee, H.-J. Kim, S.I. Seok, M.K. Nazeeruddin, M. Grätzel, High-performance nanostructured inorganic–organic heterojunction solar cells, Nano Lett. 10 (2010) 2609–2612.

[22] E. Palomares, J.N. Clifford, S.A. Haque, T. Lutz, J.R. Durrant, Control of charge recombination dynamics in dye sensitized solar cells by the use of conformally deposited metal oxide blocking layers, J. Am. Chem. Soc. 125 (2003) 475–482.

[23] S.-J. Roh, R.S. Mane, S.-K. Min, W.-J. Lee, C.D. Lokhande, S.-H. Han, Achievement of 4.51% conversion efficiency using ZnO recombination barrier layer in TiO_2 based dye-sensitized solar cells, Appl. Phys. Lett. 89 (2006) 253512.

[24] A. Zaban, S.G. Chen, S. Chappel, B.A. Gregg, Bilayer nanoporous electrodes for dye sensitized solar cells, Chem. Commun. (2000) 2231–2232.

[25] T. Taguchi, X. Zhang, I. Sutanto, K. Tokuhiro, T.N. Rao, H. Watanabe, T. Nakamori, M. Uragami, A. Fujishima, Improving the performance of solid-state dye-sensitized solar cell using MgO-coated TiO_2 nanoporous film, Chem. Commun. (2003) 2480–2481.

[26] J.Y. Kim, S. Lee, J.H. Noh, H.S. Jung, K.S. Hong, Enhanced photovoltaic properties of overlayer-coated nanocrystalline TiO_2 dye-sensitized solar cells (DSSCs), J. Electroceram. 23 (2009) 422–425.

[27] V. Ganapathy, B. Karunagaran, S.-W. Rhee, Improved performance of dye-sensitized solar cells with TiO_2/alumina core-shell formation using atomic layer deposition, J. Power Sources 195 (2010) 5138–5143.

[28] S. Ito, P. Liska, P. Comte, R. Charvet, P. Pechy, U. Bach, L. S.-Mende, S.M. Zakeeruddin, A. Kay, M.K. Nazeeruddin, M. Grätzel, Control of dark current in photoelectrochemical ($TiO_2/I^-–I_3^-$) and dye-sensitized solar cells, Chem. Commun. (2005) 4351–4353.

[29] P.M. Sommeling, B. O'Regan, R.R. Haswell, H.J.P. Smit, N.J. Bakker, J.J.T. Smits, J.M. Kroon, J.A.M. van Roosmalen, Influence of a $TiCl_4$ post-treatment on nanocrystalline TiO_2 films in dye-sensitized solar cells, J. Phys. Chem. B 110 (2006) 19191–19197.

[30] B. O'Regan, J.R. Durrant, P.M. Sommeling, N.J. Bakker, Influence of the $TiCl_4$ treatment on nanocrystalline TiO_2 films in dye-sensitized solar cells. 2. Charge density, band edge shifts, and quantification of recombination losses at short circuit, J. Phys. Chem. C 111 (2007) 14001–14010.

[31] G. Zhua, L. Pan, T. Xua, Q. Zhaob, Z. Suna, Cascade structure of TiO_2/ZnO/CdS film for quantum dot sensitized solar cells, J. Alloy Compd. 509 (2011) 7814–7818.

[32] J. Kim, H. Choi, C. Nahm, C. Kim, S. Nam, S. Kang, D.-R. Jung, J.I. Kim, J. Kang, B. Park, The role of a $TiCl_4$ treatment on the performance of CdS quantum-dot-sensitized solar cells, J. Power Sources 220 (2012) 108–113.

[33] C. Kim, J. Kim, H. Choi, C. Nahm, S. Kang, S. Lee, B. Lee, B. Park, The effect of TiO_2-coating layer on the performance in nanoporous ZnO-based dye-sensitized solar cells, J. Power Sources 232 (2013) 159–164.

[34] I. Mora-Seró, S. Giménez, F. Fabregat-Santiago, R. Gómez, Q. Shen, T. Toyoda, J. Bisquert, Recombination in quantum dot sensitized solar cells, Acc. Chem. Res. 42 (2009) 1848–1857.

[35] M. Shalom, S. Dor, S. Ruhle, L. Grinis, A. Zaban, Core/CdS quantum dot/shell mesoporous solar cells with improved stability and efficiency using an amorphous TiO_2 coating, J. Phys. Chem. C 113 (2009) 3895–3898.

[36] J.-Y. Hwang, S.-A. Lee, Y.H. Lee, S.-I. Seok, Improved photovoltaic response of nanocrystalline CdS-sensitized solar cells through interface control, Appl. Mater. Inter 2 (2010) 1343–1348.

[37] S.-M. Yang, C.-H. Huang, J. Zhai, Z.-S. Wanga, L. Jiang, High photostability and quantum yield of nanoporous TiO_2 thin film electrodes co-sensitized with capped sulfides, J. Mater. Chem. 12 (2002) 1459–1464.

[38] M. Shalom, J. Albero, Z. Tachan, E. Martínez-Ferrero, A. Zaban, E. Palomares, Quantum dot-dye bilayer-sensitized solar cells: breaking the limits imposed by the low absorbance of dye monolayers, J. Phys. Chem. Lett. 1 (2010) 1134–1138.

[39] Y. Liua, X. Suna, Q. Taia, H. Hua, B. Chena, N. Huanga, B. Seboa, X. Zhaoa, Efficiency enhancement in dye-sensitized solar cells by interfacial modification of conducting glass/mesoporous TiO_2 using a novel ZnO compact blocking film, J. Power Sources 196 (2011) 475–481.

[40] J. Xia, N. Masaki, K. Jiang, S. Yanagida, Sputtered Nb_2O_5 as a novel blocking layer at conducting glass/TiO_2 interfaces in dye-sensitized ionic liquid solar cells, J. Phys. Chem. C 111 (2007) 8092–8097.

[41] H. Choi, C. Nahm, J. Kim, J. Moon, S. Nam, C. Kim, D.-R. Jung, B. Park, The effect of $TiCl_4$-treated TiO_2 compact layer on the performance of dye-sensitized solar cell, Curr. Appl. Phys. 12 (2012) 737–741.

[42] B. Peng, G. Jungmanna, C. Jäger, D. Haarer, H.-W. Schmidt, M. Thelakkat, Systematic investigation of the role of compact TiO_2 layer in solid state dye-sensitized TiO_2 solar cells, Coord. Chem. Rev. 248 (2004) 1479–1489.

[43] S. Hore, R. Kern, Implication of device functioning due to back reaction of electrons via the conducting glass substrate in dye sensitized solar cells, Appl. Phys. Lett. 87 (2005) 263504.

[44] S.M. Waita, B.O. Aduda, J.M. Mwabora, G.A. Niklasson, C.G. Granqvist, G. Boschloo, Electrochemical characterization of TiO_2 blocking layers prepared by reactive DC magnetron sputtering, J. Electroanal. Chem. 637 (2009) 79–84.

[45] R. Hattori, H. Goto, Carrier leakage blocking effect of high temperature sputtered TiO_2 film on dye-sensitized mesoporous photoelectrode, Thin Solid Films 515 (2007) 8045–8049.

[46] H. Yu, S. Zhang, H. Zhao, G. Will, P. Liu, An efficient and low-cost TiO_2 compact layer for performance improvement of dye-sensitized solar cells, Electrochim. Acta 54 (2009) 1319–1324.

[47] M. Thelakkat, C. Schmitz, H.-Z. Schmidt, Fully vapor-deposited thin-layer titanium dioxide solar cells, Adv. Mater. 14 (2002) 577–581.

[48] J. Xia, N. Masaki, K. Jiang, S. Yanagida, Sputtered Nb_2O_5 as an effective blocking layer at conducting glass and TiO_2 interfaces in ionic liquid-based dye-sensitized solar cells, Chem. Commun. (2007) 138–140.

[49] T.-Y. Cho, S.-G. Yoon, S.S. Sekhon, M.G. Kang, C.-H. Han, The effect of a sol–gel formed TiO_2 blocking layer on the efficiency of dye-sensitized solar cells, Bull. Korean Chem. Soc. 32 (2011) 3629–3633.

[50] J. Shi, J. Liang, S. Peng, W. Xu, J. Pei, J. Chen, Synthesis, characterization and electrochemical properties of a compact titanium dioxide layer, Solid State Sci. 11 (2009) 433–438.

[51] H. Seo, M.-K. Son, J.-K. Kim, I. Shin, K. Prabakar, H.-J. Kim, Method for fabricating the compact layer in dye-sensitized solar cells by titanium sputter deposition and acid-treatments, Sol. Energy Mater. Sol. Cells 95 (2011) 340–343.

[52] B. Yoo, K.-J. Kim, S.-Y. Bang, M.J. Ko, K. Kim, N.-G. Park, Chemically deposited blocking layers on FTO substrates: effect of precursor concentration on photovoltaic performance of dye-sensitized solar cells, J. Electroanal. Chem. 638 (2010) 161–166.

[53] J. Kim, H. Choi, C. Nahm, J. Moon, C. Kim, S. Nam, D.-R. Jung, B. Park, The effect of a blocking layer on the photovoltaic performance in CdS quantum-dot-sensitized solar cells, J. Power Sources 196 (2011) 10526–10531.

[54] C. Nahm, S. Shin, W. Lee, J.I. Kim, D.-R. Jung, J. Kim, S. Nam, S. Byun, B. Park, Electronic transport and carrier concentration in conductive ZnO:Ga thin films, Curr. Appl. Phys. 13 (2013) 415–418.

[55] W. Lee, H. Kim, D.-R. Jung, J. Kim, C. Nahm, J. Lee, S. Kang, B. Lee, B. Park, An effective oxidation approach for luminescence enhancement in CdS quantum dots by H_2O_2, Nanoscale Res. Lett. 7 (2012) 672.

[56] Y. Oh, D. Ahn, S. Nam, B. Park, The effect of Al_2O_3-coating coverage on the electrochemical properties in $LiCoO_2$ thin films, J. Solid State Electrochem. 14 (2010) 1235–1240.

[57] J. Cho, T.-G. Kim, C. Kim, J.-G. Lee, Y.-W. Kim, B. Park, Comparison of Al_2O_3- and $AlPO_4$-coated $LiCoO_2$ cathode materials for a Li-ion cell, J. Power Sources 146 (2005) 58–64.

[58] Y.J. Kim, H. Kim, B. Kim, D. Ahn, J.-G. Lee, T.-J. Kim, D. Son, J. Cho, Y.-W. Kim, B. Park, Electrochemical stability of thin-film $LiCoO_2$ cathodes by aluminum-oxide coating, Chem. Mater. 15 (2003) 1505–1511.

[59] Y.J. Kim, J. Cho, T.-J. Kim, B. Park, Suppression of cobalt dissolution from the $LiCoO_2$ cathodes with various metal-oxide coatings, J. Electrochem. Soc. 150 (2003) A1723–A1725.

[60] Y.J. Kim, T.-J. Kim, J.W. Shin, B. Park, J. Cho, The effect of Al_2O_3 coating on the cycle-life performance in thin-film $LiCoO_2$ cathodes, J. Electrochem. Soc. 149 (2002) A1337–A1341.

[61] Z. Wang, L. Liu, L. Chen, X. Huang, Structural and Electrochemical characterizations of surface-modified $LiCoO_2$ cathode materials for Li-ion batteries, Solid State Ionics 148 (2002) 335–342.

[62] J. Cho, Y.J. Kim, T.-J. Kim, B. Park, Effect of Al_2O_3-coated *o*-$LiMnO_2$ cathodes prepared at various temperatures on the 55 °C cycling behavior, J. Electrochem. Soc. 149 (2002) A127–A132.

[63] J. Cho, Y.J. Kim, B. Park, $LiCoO_2$ cathode material that does not show a phase transition from hexagonal to monoclinic phase, J. Electrochem. Soc. 148 (2001) A1110–A1115.

[64] J. Cho, T.-J. Kim, B. Park, The effect of a metal-oxide coating on the cycling behavior at 55 °C in orthorhombic $LiMnO_2$ cathode materials, J. Electrochem. Soc. 149 (2002) A288–A292.

[65] J. Cho, Y.J. Kim, T.-J. Kim, B. Park, Enhanced structural stability of *o*-$LiMnO_2$ by sol–gel coating of Al_2O_3, Chem. Mater. 13 (2001) 18–20.

[66] M.M. Thackeray, C.S. Johnson, J. Kim, K.C. Lauzze, J.T. Vaughey, N. Dietz, D. Abraham, S.A. Hackney, W. Zeltner, M.A. Anderson, ZrO_2- and Li_2ZrO_3-stabilized spinel and layered electrodes for lithium batteries, Electrochem. Commun. 5 (2003) 752–758.

[67] J. Cho, T.-J. Kim, Y.J. Kim, B. Park, Complete blocking of Mn^{3+} ion dissolution from $LiMn_2O_4$ spinel intercalation compound by Co_3O_4 coating, Chem. Commun. (2001) 1074–1075.

[68] J. Cho, Y.J. Kim, B. Park, Novel $LiCoO_2$ cathode material with Al_2O_3 coating for a Li ion cell, Chem. Mater. 12 (2000) 3788–3791.

[69] S. Myung, K. Izumi, S. Komaba, Y. Sun, H. Yashiro, N. Kumagai, Role of alumina coating on Li–Ni–Co–Mn–O particles as positive electrode material for lithium-ion batteries, Chem. Mater. 17 (2005) 3695–3704.

[70] S. Nam, S. Kim, S. Wi, H. Choi, S. Byun, S.-M. Choi, S.-I. Yoo, K.T. Lee, B. Park, The role of carbon incorporation in SnO_2 nanoparticles for Li rechargeable batteries, J. Power Sources 211 (2012) 154–160.

[71] J. Cho, Y.J. Kim, T.-J. Kim, B. Park, Zero-strain intercalation cathode for rechargeable Li-ion cell, Angew. Chem. Int. Ed. 40 (2001) 3367–3369.

[72] B. Kim, C. Kim, D. Ahn, T. Moon, J. Ahn, Y. Park, B. Park, Nanostructural effect of $AlPO_4$-nanoparticle coating on the cycle-life performance in $LiCoO_2$ thin films, Electrochem. Solid-State Lett. 10 (2007) A32–A35.

[73] B. Kim, C. Kim, T.-G. Kim, D. Ahn, B. Park, The effect of $AlPO_4$-coating layer on the electrochemical properties in $LiCoO_2$ thin films, J. Electrochem. Soc. 153 (2006) A1773–A1777.

[74] S. Verdier, L.E. Ouatani, R. Dedryvre, F. Bonhomme, P. Biensan, D. Gonbeau, XPS study on Al_2O_3- and $AlPO_4$-coated $LiCoO_2$ cathode material for high-capacity Li-ion batteries, J. Electrochem. Soc. 154 (2007) A1088–A1099.

[75] T.-J. Kim, D. Son, J. Cho, B. Park, H. Yang, Enhanced electrochemical properties of SnO_2 anode by $AlPO_4$ coating, Electrochim. Acta 49 (2004) 4405–4410.

[76] J.-G. Lee, B. Kim, J. Cho, Y.-W. Kim, B. Park, Effect of $AlPO_4$-nanoparticle coating concentration on the high-cutoff-voltage electrochemical performances in $LiCoO_2$, J. Electrochem. Soc. 151 (2004) A801–A805.

[77] J. Cho, Y.-W. Kim, B. Kim, J.-G. Lee, B. Park, A breakthrough in the safety of lithium secondary batteries by coating the cathode material with $AlPO_4$ nanoparticles, Angew. Chem. Int. Ed. 42 (2003) 1618–1621.

[78] A.T. Appapillai, A.N. Mansour, J. Cho, Y. Shao-Horn, Microstructure of $LiCoO_2$ with and without $AlPO_4$ nanoparticle coating: combined STEM and XPS studies, Chem. Mater. 19 (2007) 5748–5757.

[79] J. Cho, J.-G. Lee, B. Kim, B. Park, Effect of P_2O_5 and $AlPO_4$ coating on $LiCoO_2$ cathode material, Chem. Mater. 15 (2003) 3190–3193.

[80] T. Moon, C. Kim, S.-T. Hwang, B. Park, Electrochemical properties of disordered-carbon-coated SnO_2 nanoparticles for Li rechargeable batteries, Electrochem. Solid-State Lett. 9 (2006) A408–A411.

[81] Y. Oh, S. Nam, S. Wi, S. Hong, B. Park, Review paper: nanoscale interface control for high-performance Li-ion batteries, Electron. Mater. Lett. 8 (2012) 91–105.

[82] Y. Oh, D. Ahn, S. Nam, C. Kim, J.-G. Lee, B. Park, The enhancement of cycle-life performance in $LiCoO_2$ thin film by partial Al_2O_3 coating, Electron. Mater. Lett. 4 (2008) 103–105.

[83] S. Wi, S. Nam, Y. Oh, J. Kim, H. Choi, S. Hong, S. Byun, S. Kang, D.J. Choi, K. Ahn, Y.-H. Kim, B. Park, Facile synthesis of porous-carbon/$LiFePO_4$ nanocomposites, J. Nanopart. Res. 14 (2012) 1327.

[84] S. Nam, S. Wi, C. Nahm, H. Choi, B. Park, Challenges in synthesizing carbon-coated $LiFePO_4$ nanoparticles from hydrous $FePO_4$ and their electrochemical properties, Mater. Res. Bull. 47 (2012) 3495–3498.

[85] Y. Oh, J. Kang, S. Nam, S. Byun, B. Park, Pt/$AlPO_4$ nanocomposite thin-film electrodes for ethanol electrooxidation, Mater. Chem. Phys. 135 (2012) 188–192.

[86] Y. Park, B. Lee, C. Kim, J. Kim, S. Nam, Y. Oh, B. Park, Modification of gold catalysis with aluminum phosphate for oxygen-reduction reaction, J. Phys. Chem. C 114 (2010) 3688–3692.

[87] C. Kim, B. Lee, Y. Park, B. Park, J. Lee, H. Kim, Iron-phosphate/platinum/carbon nanocomposites for enhanced electrocatalytic stability, Appl. Phys. Lett. 91 (2007) 113101.

[88] S.-K. Wang, F. Tseng, T.-K. Yeh, C.-C. Chieng, Electrocatalytic properties improvement on carbon-nanotubes coated reaction surface for micro-DMFC, J. Power Sources 167 (2007) 413–419.

[89] Y. Park, B. Lee, C. Kim, J. Kim, B. Park, Effects of iron–phosphate coating on Ru dissolution in the PtRu thin-film electrodes, J. Mater. Res. 24 (2009) 140–144.

[90] Y. Park, B. Lee, C. Kim, Y. Oh, S. Nam, B. Park, The effects of ruthenium-oxidation states on Ru dissolution in PtRu thin-film electrodes, J. Mater. Res. 24 (2009) 2762–2766.

[91] A.A. Aal, H.B. Hassan, M.A.A. Rahim, Nanostructured Ni–P–TiO_2 composite coatings for electrocatalytic oxidation of small organic molecules, J. Electroanal. Chem. 619 (2008) 17–25.

[92] C. Nahm, C. Kim, Y. Park, B. Park, Nanoporous Pt thin films with superior catalytic activities by the electrochemical dissolution of Al, Met. Mater. Int. 15 (2009) 989–992.

[93] S.M. Alia, K.O. Jensen, B.S. Pivovar, Y. Yan, Platinum-coated palladium nanotubes as oxygen reduction reaction electrocatalysts, ACS Catal. 2 (2012) 858–863.

[94] C. Kim, Y. Park, C. Nahm, B. Park, Formation of nanoporous Pt thin films by electrochemical dissolution, Electron. Mater. Lett. 4 (2008) 75–77.

[95] C. Nahm, C. Kim, Y. Park, B. Lee, B. Park, Iron-phosphate/Pt nanostructured electrodes for high-efficiency fuel cells, Electron. Mater. Lett. 4 (2008) 5–7.

[96] Y. Lin, H. Li, C. Liu, W. Xing, X. Ji, Surface-modified Nafion membranes with mesoporous SiO_2 layers via a facile dip-coating approach for direct methanol fuel cells, J. Power Sources 185 (2008) 904–908.

[97] J. Park, Y. Oh, Y. Park, S. Nam, J. Moon, J. Kang, D.-R. Jung, S. Byun, B. Park, Methanol oxidation in nanostructured platinum/cerium-phosphate thin films, Curr. Appl. Phys. 11 (2011) S2–S5.

[98] Y. Park, S. Nam, Y. Oh, H. Choi, J. Park, B. Park, Electrochemical promotion of oxygen reduction on gold with aluminum-phosphate overlayer, J. Phys. Chem. C 115 (2011) 7092–7096.

[99] S. Nishimura, N. Abrams, B.A. Lewis, L.I. Halaoui, T.E. Mallouk, K.D. Benkstein, J. Lagemaat, A.J. Frank, Standing wave enhancement of red absorbance and photocurrent in dye-sensitized titanium dioxide photoelectrodes coupled to photonic crystals, J. Am. Chem. Soc. 125 (2003) 6306–6310.

[100] Q. Zhang, T.P. Chou, B. Russo, S.A. Jenekhe, G. Cao, Polydisperse aggregates of ZnO nanocrystallites: a method for energy-conversion-efficiency enhancement in dye-sensitized solar cells, Adv. Funct. Mater. 18 (2008) 1654–1660.

[101] Q. Zhang, T.P. Chou, B. Russo, S.A. Jenekhe, G. Cao, Aggregation of ZnO nanocrystallites for high conversion efficiency in dye-sensitized solar cells, Angew. Chem. Int. Ed. 47 (2008) 2402–2406.

[102] T.P. Chou, Q.F. Zhang, G.E. Fryxell, G. Cao, Hierarchically structured ZnO film for dye-sensitized solar cells with enhanced energy conversion efficiency, Adv. Mater. 19 (2007) 2588–2592.

[103] Q. Zhang, C.S. Dandeneau, X. Zhou, G. Cao, ZnO nanostructures for dye-sensitized solar cells, Adv. Mater. 21 (2009) 4087–4108.

[104] H.-J. Koo, J. Park, B. Yoo, K. Yoo, K. Kim, N.-G. Park, Size-dependent scattering efficiency in dye-sensitized solar cell, Inorg. Chim. Acta 361 (2008) 677–683.

[105] J. Xi, Q. Zhang, K. Park, Y. Sun, G. Cao, Enhanced power conversion efficiency in dye-sensitized solar cells with TiO_2 aggregates/nanocrystallites mixed photoelectrodes, Electrochim. Acta 56 (2011) 1960–1966.

[106] S.D. Standridge, G.C. Schatz, J.T. Hupp, Toward plasmonic solar cells: protection of silver nanoparticles via atomic layer deposition of TiO_2, Langmuir 25 (2009) 2596–2600.

[107] S.D. Standridge, G.C. Schatz, J.T. Hupp, Distance dependence of plasmon-enhanced photocurrent in dye-sensitized solar cells, J. Am. Chem. Soc. 131 (2009) 8407–8409.

[108] J.I. Kim, D.-R. Jung, J. Kim, C. Nahm, S. Byun, S. Lee, B. Park, Surface-plasmon-coupled photoluminescence from CdS nanoparticles with Au films, Solid State Commun. 152 (2012) 1767–1770.

[109] D.-R. Jung, J. Kim, C. Nahm, S. Nam, J.I. Kim, B. Park, Surface-plasmon-enhanced photoluminescence of CdS nanoparticles with Au/SiO_2 nanocomposites, Mater. Res. Bull. 47 (2012) 453–457.

[110] M.D. Brown, T. Suteewong, R.S.S. Kumar, V. D'Innocenzo, A. Petrozza, M.M. Lee, U. Wiesner, H.J. Snaith, Plasmonic dye-sensitized solar cells using core-shell metal–insulator nanoparticles, Nano Lett. 11 (2011) 438–445.

[111] C. Nahm, H. Choi, J. Kim, D.-R. Jung, C. Kim, J. Moon, B. Lee, B. Park, The effects of 100 nm-diameter Au nanoparticles on dye-sensitized solar cells, Appl. Phys. Lett. 99 (2011) 253107.

[112] H.A. Atwater, A. Polman, Plasmonics for improved photovoltaic devices, Nat. Mater. 9 (2010) 205–213.

[113] D.-R. Jung, J. Kim, S. Nam, C. Nahm, H. Choi, J.I. Kim, J. Lee, C. Kim, B. Park, Photoluminescence enhancement in CdS nanoparticles by surface-plasmon resonance, Appl. Phys. Lett. 99 (2011) 041906.

[114] J. Kim, H. Choi, C. Nahm, B. Park, Review paper: surface plasmon resonance for photoluminescence and solar-cell applications, Electron. Mater. Lett. 8 (2012) 351–364.

[115] D.-R. Jung, J. Kim, C. Nahm, H. Choi, S. Nam, B. Park, Review paper: semiconductor nanoparticles with surface passivation and surface plasmon, Electron. Mater. Lett. 7 (2011) 185–194.

[116] A. Nattestad, A.J. Mozer, M.K.R. Fischer, Y.-B. Cheng, A. Mishra, P. Bäuerle, U. Bach, Highly efficient photocathodes for dye-sensitized tandem solar cells, Nat. Mater. 9 (2010) 31–35.

[117] Z. Bian, T. Tachikawa, S.-C. Cui, M. Fujitsuka, T. Majima, Single-molecule charge transfer dynamics in dye-sensitized p-type NiO solar cells: influences of insulating Al_2O_3 layers, Chem. Sci. 3 (2012) 370–379.

[118] H. Yang, G.H. Guai, C. Guo, Q. Song, S.P. Jiang, Y. Wang, W. Zhang, C.M. Li, NiO/graphene composite for enhanced charge separation and collection in p-type dye sensitized solar cell, J. Phys. Chem. C 115 (2011) 12209–12215.

[119] X.L. Zhang, F. Huang, A. Nattestad, K. Wang, D. Fu, A. Mishra, P. Bäuerle, U. Bach, Y.-B. Cheng, Enhanced open-circuit voltage of p-type DSC with highly crystalline NiO nanoparticles, Chem. Commun. 47 (2011) 4808–4810.

[120] G. Natu, Z. Huang, Z. Ji, Y. Wu, The effect of an atomically deposited layer of alumina on NiO in p-type dye-sensitized solar cells, Langmuir 28 (2012) 950–956.

[121] J. He, H. Lindström, A. Hagfeldt, S.-E. Lindquist, Dye-sensitized nanostructured tandem cell-first demonstrated cell with a dye-sensitized photocathode, Sol. Energy Mater. Sol. Cells 62 (2000) 265–273.

[122] A. Morandeira, G. Boschloo, A. Hagfeldt, L. Hammarström, Photoinduced ultrafast dynamics of coumarin 343 sensitized p-type-nanostructured NiO films, J. Phys. Chem. B 109 (2005) 19403–19410.

[123] F. Odobel, Y. Pellegrin, E.A. Gibson, A. Hagfeldt, A.L. Smeigh, L. Hammarström, Recent advances and future directions to optimize the performances of p-type dye-sensitized solar cells, Coord. Chem. Rev. 256 (2012) 2414–2423.

[124] T. Berger, T. Lana-Villarreal, D. Monllor-Satoca, R. Gómez, An electrochemical study on the nature of trap states in nanocrystalline rutile thin films, J. Phys. Chem. C 111 (2007) 9936–9942.

[125] Z. Zhang, S.M. Zakeeruddin, B. O'Regan, R. Humphry-Baker, M. Grätzel, Influence of 4-guanidinobutyric acid as coadsorbent in reducing recombination in dye-sensitized solar cells, J. Phys. Chem. B 109 (2005) 21818–21824.

[126] A. Zaban, M. Greenshtein, J. Bisquert, Determination of the electron lifetime in nanocrystalline dye solar cells by open-circuit voltage decay measurements, ChemPhysChem 4 (2003) 859–864.

[127] J. Bisquert, A. Zaban, M. Greenshtein, I. Mora-Seró, Determination of rate constants for charge transfer and the distribution of semiconductor and electrolyte electronic energy levels in dye-sensitized solar cells by open-circuit photovoltage decay method, J. Am. Chem. Soc. 126 (2004) 13550–13559.

[128] T. Miyasaka, Toward printable sensitized mesoscopic solar cells: light-harvesting management with thin TiO_2 films, J. Phys. Chem. Lett. 2 (2011) 262–269.
[129] G. Kron, U. Rau, M. Dürr, T. Miteva, G. Nelles, A. Yasuda, J.H. Werner, Diffusion limitations to I_3^-/I^- electrolyte transport through nanoporous TiO_2 networks, Electrochem. Solid-State Lett. 6 (2003) E11–E114.
[130] Q. Wang, J.-E. Moser, M. Grätzel, Electrochemical impedance spectroscopic analysis of dye-sensitized solar cells, J. Phys. Chem. B 109 (2005) 14945–14953.
[131] K. Zhu, S.-R. Jang, A.J. Frank, Impact of high charge-collection efficiencies and dark energy-loss processes on transport, recombination, and photovoltaic properties of dye-sensitized solar cells, J. Phys. Chem. Lett. 2 (2011) 1070–1076.
[132] Y.J. Kim, M.H. Lee, H.J. Kim, G. Lim, Y.S. Choi, N.-G. Park, K. Kim, W.I. Lee, Formation of highly efficient dye-sensitized solar cells by hierarchical pore generation with nanoporous TiO_2 spheres, Adv. Mater. 21 (2009) 3668–3673.
[133] J.-Y. Lee, P. Peumans, The origin of enhanced optical absorption in solar cells with metal nanoparticles embedded in the active layer, Opt. Express 18 (2010) 10078–10087.
[134] K. Tanabe, Field enhancement around metal nanoparticles and nanoshells: a systematic investigation, J. Phys. Chem. C 112 (2008) 15721–15728.
[135] D. Adler, J. Feinleib, Electrical and optical properties of narrow-band materials, Phys. Rev. B 2 (1970) 3112–3134.
[136] H. Sato, T. Minami, S. Takata, T. Yamada, Transparent conducting p-type NiO thin films prepared by magnetron sputtering, Thin Solid Films 236 (1993) 27–31.
[137] E.L. Miller, R.E. Rocheleau, Electrochemical and electrochromic behavior of reactively sputtered nickel oxide, J. Electrochem. Soc. 144 (1997) 1995–2003.
[138] S. Mori, S. Fukuda, S. Sumikura, Y. Takeda, Y. Tamaki, E. Suzuki, T. Abe, Charge-transfer processes in dye-sensitized NiO solar cells, J. Phys. Chem. C 112 (2008) 16134–16139.
[139] E.A. Gibson, A.L. Smeigh, L.L. Pleux, J. Fortage, G. Boschloo, E. Blart, Y. Pellegrin, F. Odobel, A. Hagfeldt, L. Hammarström, A p-type NiO-based dye-sensitized solar cell with an open-circuit voltage of 0.35 V, Angew. Chem. Int. Ed. 48 (2009) 4402–4405.
[140] Z. Huang, G. Natu, Z. Ji, P. Hasin, Y. Wu, p-type dye-sensitized NiO solar cells: a study by electrochemical impedance spectroscopy, J. Phys. Chem. C 115 (2011) 25109–25114.